

## Interaction Model of Rainfall, Lake, and Ground Waters

Elroy Koyari<sup>1\*</sup>, M. Bisri<sup>2\*</sup>, Dian Sisingih<sup>2</sup>, Runi Asmaranto<sup>2</sup>

<sup>1</sup> Doctoral Program at the Department of Civil Engineering, Faculty of Engineering, University of Brawijaya, Jl. MT Haryono No 167 Malang, Indonesia

<sup>2</sup> Department of Water Resources, Faculty of Engineering, University of Brawijaya, Jl. MT Haryono No 167 Malang, Indonesia

**Abstract:** This research intends to build an interaction model between rainfall, lake water, and ground water. The location of research is in the Sentani Lake where is placed in the Jayapura Regency-Papua-Indonesia. Sentani Lake is a lake in the Sentani Watershed. Sentani Lake is located between Jayapura City and Jayapura Regency-Papua Province. The area of Sentani Lake is 9,630 ha with the depth is 75 m over the sea. In the northern of this lake are the Cyclops Mountains (Dafonsero) that separate the Sentani Lake and the Pacific Sea. The Sentani Lake functions as the track of transportation, food source, drinking water source, and tourism. Based on the bathymetry analysis result which is obtained from the River Region Institution of Papua, the Sentani Lake has the smallest elevation from 13.05 mdpl until 71.5 mdpl with a maximum storage capacity of 4.8 milliard m<sup>3</sup>. The methodology of this research consists of 1) To set and to simulate of Hydrology Model; 2) Analysis of water balance; 3) To set up the hydro-geology model; 4) To simulate the integration of rainfall-lake water- ground water. The interaction model between rainfall and lake waters is built based on the relation between the outlet discharge and the rainfall at 10 points and then is validated at the 5 points of observation data. This model produces the formulation as follows: inflow to the lake from rainfall =  $0.067 \times \text{rainfall} - 5$ . The interaction model between the lake water level and the ground water level is built based on the value of ground water-level fluctuation and the lake water level at the 10 points, and it is validated at the 6 points of observation data. This model produces the following formulation: fluctuation of ground water level =  $0.1529 \times \text{fluctuation of lake water level}$ . By combining the ground water and run-off in the Sentani Watershed, it is known as follows: inflow total of lake = base-flow +  $0.067 \times \text{rainfall} - 5$ .

**Keywords:** lake, rainfall, lake water, ground water.

## 降雨、湖泊和地下水的相互作用模型

**摘要:** 本研究旨在建立降雨、湖水和地下水之间的相互作用模型。研究地点在位于印度尼西亚巴布亚查亚普拉摄政区的森塔尼湖中。仙谷湖是仙谷流域的一个湖泊。仙谷湖位于查亚普拉市和查亚普拉摄政-巴布亚省之间。仙谷湖面积 9,630 公顷, 海深 75 米。在这个湖的北部是独眼巨人山脉(达丰塞罗), 它将仙谷湖和太平洋分开。仙谷湖作为交通、食物来源、饮用水来源和旅游的轨道。根据巴布亚河区研究所获得的测深分析结果, 仙谷湖的海拔最低, 为 13.05 mdpl 至 71.5 mdpl, 最大蓄水量为 4.8 毫立方米。本研究的方法包括 1) 水文模型的设置和模拟; 2) 水平衡分析; 3) 建立水文地质模型; 4) 模拟降雨-湖泊水-地下水的整合。根据出水口流量与 10 个点降雨量的关系建立降雨与湖水交互作用模型, 并在 5 个点观测数据上进行验证。该模型产生公式为: 降雨入湖量 =  $0.067 \times \text{降雨量} - 5$ 。湖泊水位与地下水水位的交互作用模型是根据地下水位波动值和湖水量建立的 10 个点的水平, 并在 6 个点的观测数据上得到验证。该模型产生以下公式: 地下水位波动 =  $0.1529 \times \text{湖水位波动}$ 。通过将仙谷流域的地下水和径流结合起来, 已知如下: 湖泊总流入量 = 基流 +  $0.067 \times \text{降雨量} - 5$ 。

Received: June 16, 2022 / Revised: July 11, 2022 / Accepted: August 8, 2022 / Published: September 30, 2022

About the authors: Elroy Koyari, Doctoral Program at the Department of Civil Engineering, Faculty of Engineering, University of Brawijaya, Malang, Indonesia; M. Bisri, Dian Sisingih, Runi Asmaranto, Department of Water Resources, Faculty of Engineering, University of Brawijaya, Malang, Indonesia

Corresponding authors Elroy Koyari, [elroykoyari@yahoo.co.id](mailto:elroykoyari@yahoo.co.id); M. Bisri, [mbisri@ub.ac.id](mailto:mbisri@ub.ac.id)

关键词：湖，降雨，湖水，地下水。

## 1. Introduction

The impact of human activities on the ecosystems has long been recognized, and there is increasing the evidence to support the indicator that we have entered the anthropogenic period [1]. Some human activities have been documented and recorded as one of the main driving forces that are simultaneously changes in the natural environment [2], the landscape spatial pattern [3, 4], and goods and service availability in the ecosystem [5]. The problems about the inundation and flooding are more critical generally because of the climate change and, specifically, change in the rainfall intensity [6].

In 2013, the height increasing of Sentani lake water level was 1–2 m and caused area inundation in surrounding Sentani Lake. According to the environment agency in the United Kingdom, the lake water level increased if there was the extreme rainfall, so the soil and geology became saturated and caused the ground water level to rise, and the lake water level was increasing [11]. The ground water and lake water can impact one another from the quantity and quality side [7]. The main factor that affects the fluctuation of the lake water level is necessary to be analyzed through the integrated simulation between rainfall-lake water-ground water.

The other analysis mentioned that, in the Sentani Watershed, mainly in the Sentani Lake, the increasing water level is caused by the high rainfall, big erosion speed, and the slope gradient in the Sentani Lake that is more than 5%. This condition causes the erosion and sedimentation that gives impact on the increasing Sentani Lake water level [8]. The other researcher said that the increasing critical area and high rainfall intensity in the upstream of Sentani Lake can cause the increasing of lake water height because the rainfall flow in the upstream will enter as the inflow into Sentani Lake. The increase of critical area plays a critical role in forming the run-off because it can change the other hydrology processes, such as infiltration, evapotranspiration, interception, and erosion [9].

To evaluate the change in forming the run-off on a spatial and temporal scale, an analysis of land use change is very needed [3, 10] that recommend the use combination of hydrology model and traditional statistical tests to analyze the impact of land use change on the run-off in the water catchment scale. However, this research will analyze the much-influenced component in the increasing of Sentani Lake water level through the approach of numerical simulation and water balance.

## 2. Material and Method

### 2.1. Research Location

Sentani Lake is located in the Jayapura Regency-Papua-Indonesia. Sentani Lake is located between Jayapura City and Jayapura Regency-Papua Province with the coordinate is in the east longest of  $140^{\circ}23'$ – $140^{\circ}50'$  and south longest of  $2^{\circ}31'$ – $2^{\circ}41'$ LS (Fig. 1 and 2).

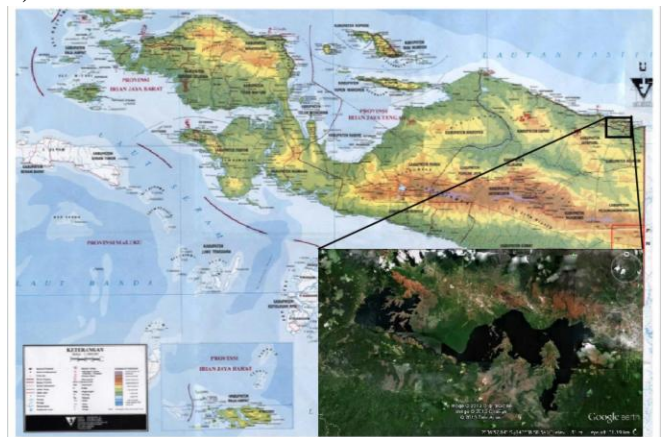


Fig. 1 Location of Sentani Lake

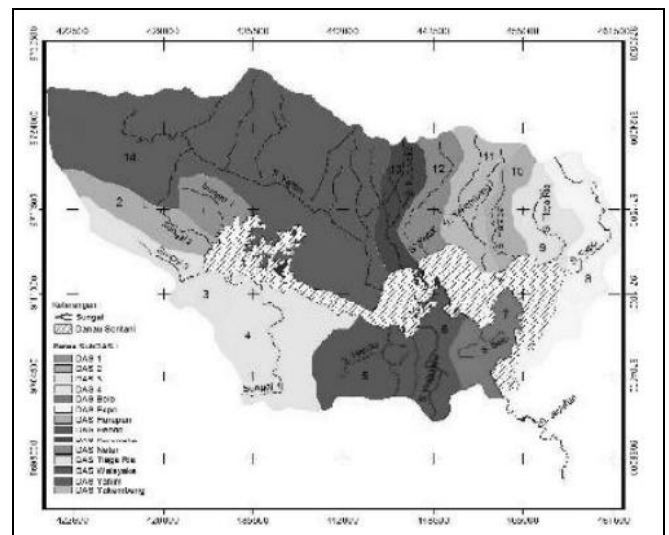


Fig. 2 Watershed map in the surroundings of Sentani Lake

### 2.2. Research Methodology

This research consists of five steps: 1) Literature study; 2) Data collection; 3) Field survey; 4) Data analysis; 5) Development of model and simulation.

### 2.3. Analysis of Design Flood

The design flood is analyzed in the Sentani Lake Watershed. The scheme used is the same as the analysis of water availability except the parameter of losses. The analysis of losses actually uses the same

parameter as the water availability analysis method using the same Curve Number value (CN), only the analysis is different such as using the parameter of initial abstraction (Ia) with the formulation as follows:

$$Ia = 0,2 \left( \frac{25.400 - 254 CN}{CN} \right) \quad (1)$$

However, the base-flow is using the recession parameter and the ratio to the peak. This parameter is used to determine the form of the flood hydrograph at the study location. The different value of recession is connected with the provision. This range can be seen as in Table 1. However, the value of ratio to peak is obtained by trial and error regarding the hydrograph form that is desired.

Table 1 Value range of the recession

Flow Component	Recession Constant, Daily
Groundwater	0.95
Interflow	0.8-0.9
Surface runoff	0.3-0.8

## 2.4. Numeric Simulation between Lake and Ground Waters

The numeric simulation between the lake water and ground water is carried out using the Modflow. Modflow is a three-dimensional ground water numeric model that uses the finite difference (based on the Darcy Law and Fluid Mass Eternity Law) to simulate the saturated flow. As the grid-based model, the analysis is carried out in the point that is located in the middle of every grid (Fig. 3).

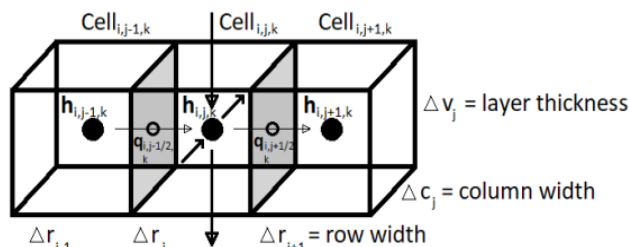


Fig. 3 Flowchart of box center indicates how the Modflow carries out the analysis

The equation of finite difference is evaluated in the point that is located in the cell center, in the three dimension directions for determining the inflow and outflow flux. In the Modflow, the ground water flow is regulated with the fluid mass eternity law as follows:

$$-\frac{\partial v_x}{\partial x} - \frac{\partial v_y}{\partial y} - \frac{\partial v_z}{\partial z} = S_s \frac{\partial h}{\partial t} \quad (2)$$

where  $v$  is the velocity,  $h$  is the hydraulic head,  $t$  is the time, and  $S_s$  is the specific storage in the pore media. The Darcy Law is as follows:

$$v_x = -K_x \frac{\partial h}{\partial x} \quad (3)$$

where  $K$  is the hydraulic conductivity for pore media. The equation of ground water flow in the  $x$ ,  $y$ , and  $z$  directions is presented with the following equation:

$$\frac{\partial}{\partial x} \left( K_{xx} \frac{\partial h}{\partial x} \right) + \frac{\partial}{\partial y} \left( K_{yy} \frac{\partial h}{\partial y} \right) + \frac{\partial}{\partial z} \left( K_{zz} \frac{\partial h}{\partial z} \right) + W = S_s \frac{\partial h}{\partial t} \quad (4)$$

In the equation above,  $K$  changes the  $v$ , and  $W$  shows an external factor like a pump well. If the infinitesimal difference ( $dx, dy, dz$ ) is changed with the finite difference ( $\Delta x, \Delta y, \Delta z$ ), the equation for  $x$ -direction is as the following:

$$\frac{\partial}{\partial x} \left( K_{xx} \frac{\partial h}{\partial x} \right) = \frac{1}{\Delta x} \left( K_{i+1/2} \frac{(h_{i+1} - h_i)}{\Delta x_{i+1/2}} - K_{i-1/2} \frac{(h_i - h_{i-1})}{\Delta x_{i-1/2}} \right) \quad (5)$$

## 3. Results and Discussion

### 3.1. Interaction Conceptual Model of Lake and Ground Waters

The conceptual model is built based on the geology and hydro-geology condition. This model is built by entering the topography, hydraulic conductivity value of the layer, and boundary condition in the software of Modflow. Geologically, the survey area plan (Fig. 4) that is Yalimo Regency-Papua in the geology map of Lembar Rotanburg/Idenburg Barat-Irian Jaya is located in the Kambelangan stone group and is not separated from the specific type of mud or clay limestone.

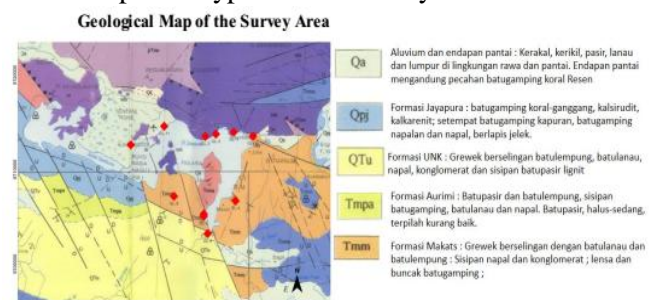


Fig. 4 Geo-electric survey locations

Based on the interpretation result of geo-electric data in the first location (Fig. 4), the resistivity value of stone in this location is approximately 0-537 ohm.m. The resistivity value of stone in the range 3–25 ohm.m is interpreted as silt, however, in the range 15–300 ohm.m is interpreted as sand. Based on the regional geology map, the stone in this area is as the alluvium layer that is dominated by sand and silt. At points GL-10 and GL-1, the first layer is the topsoil. The second layer is dominated by clay, and the third one is the sandy layer. At points GL-3 and GL-11, the first layer is the topsoil, the second one is clay with the thickness between 1 and 9 m, and the third one is a sandy layer with the thickness between 56 and 87 m. In the point GL-11, the first layer is as the cover layer, the second one is the interlude between sand and silt, and the third one is dominated by silt. In the point GL-9, the first layer is as the cover layer, the second one is dominated by silt with the depth between 1 and 71 m, and the third one is a sand layer with the depth between 71 and 100 m (Fig. 5).

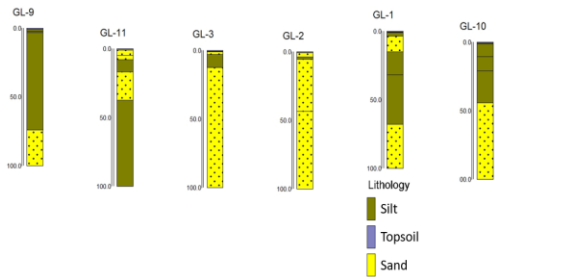


Fig. 5 Geo-electric section: Points GL-9, GL-11, GL-3, GL-2, GL-1, and GL-10

The second location consists of points GL-4, GL-5, GL-6, GL-7, and GL-8. The resistivity value of stone in this location is in the range 0–145 ohm.m. At points GL-4 and GL-6, the first layer is the cover layer, the second one is dominated by sand, and the third one is dominated by silt with the thickness between 60 and 70 m. At points GL-5 and GL-6, the first layer is the cover layer, the second one is silt with the thickness is 5, the third one is sand with the thickness between 30 and 40 m, and the fourth one is silt with the thickness is 50 m. In the point GL-8, the first layer is the cover layer, the second one is silt with the thickness is 40 m, the third one is sand with the thickness is 60 m (Fig. 6).

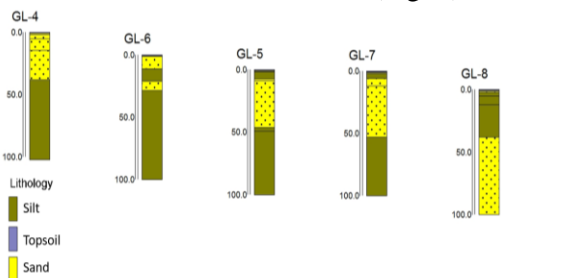


Fig. 6 Geo-electric section at Points GL-4, GL-6, GL-5, GL-7, and GL-8

The interpretation of geo-electric data shows that in the northern of Sentani Lake, the upper layer is dominated by silt except in the point GL-3 and GL-2. However, in the lower one is as the sandy layer. This location is the part of alluvium formation that consists of arm, gravel, sandy gravel, and silt. In the southern part, the upper layer is sand, and then the lower part is dominated by a sandy layer. This location is as the part of the Makats formation that consists of Grewek, which is interspersed with silt stone and clay stone. Fig. 7 is a section of the three-dimensional geo-electric point.

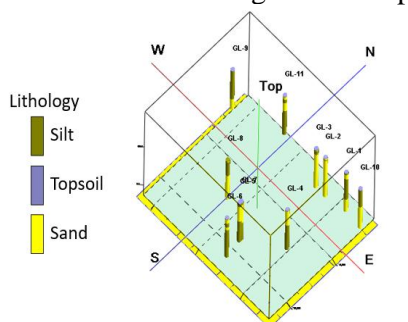


Fig. 7 Three-dimensional section of geo-electric point in the Sentani Lake area

Generally, the topography of the research location supports the ground water and lake water flow, concentrated in the Sentani Lake. Based on the regional geology map and the value of hydraulic conductivity for the stone layer in this research location is classified into 3 such as order 10–4 for alluvial, order 10–5 for sandy stone, and order 10–9 for Melange and frozen stone (Fig. 8). As the aim of the research is to know the pattern of ground water – lake water fluctuation, so the boundary condition that is used in Sentani Lake is the constant head for this model. However, the other research that is carried out by [13] uses the lake boundary condition for a lake.

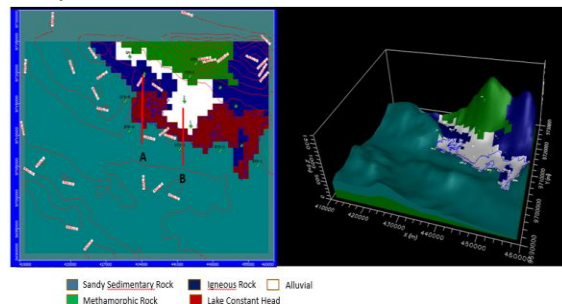
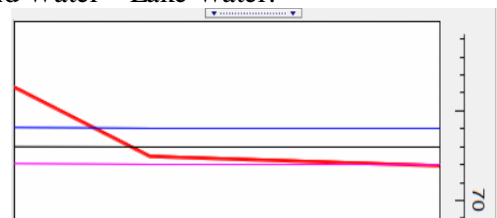


Fig. 8 Hydro-geological conceptual model of Sentani Lake

The fluctuation pattern of ground water level follows the fluctuation of Lake water level in the low land area surrounding Sentani Lake. It agrees with the research of [14] that the transient ground water fluctuates with the lake water level, so there is happen the cross. Part of [14] is determined in the flat land in surrounding Sentani Lake. The fluctuation pattern of ground water level – lake water level is analyzed through 3 scenarios that are the scenario-1 if the lake water level is down to 1 m, the scenario-2 if the lake water level is normal, and scenario-3 if the lake water level is on the land surface. From the section of the three scenarios in the Fig. 9 and 10, it is seen that the higher lake water level causes the higher ground water level. Then, the fluctuation pattern is observed in the northern flat land and southern Sentani Lake that have the different stone.

The north lookout B that has the alluvial lithology experiences more dynamic the ground water fluctuation and it follows the lake water level because it has higher hydraulic conductivity. This agrees with the simulation of a constant head lake in an alluvial aquifer by [15]. Fig. 9 presents the interaction section Ground Water – Lake Water +1 (a) Normal Lake Water (b) Lake Water -1 (c) and Fig. 10 presents the interaction pattern of Ground Water – Lake Water.



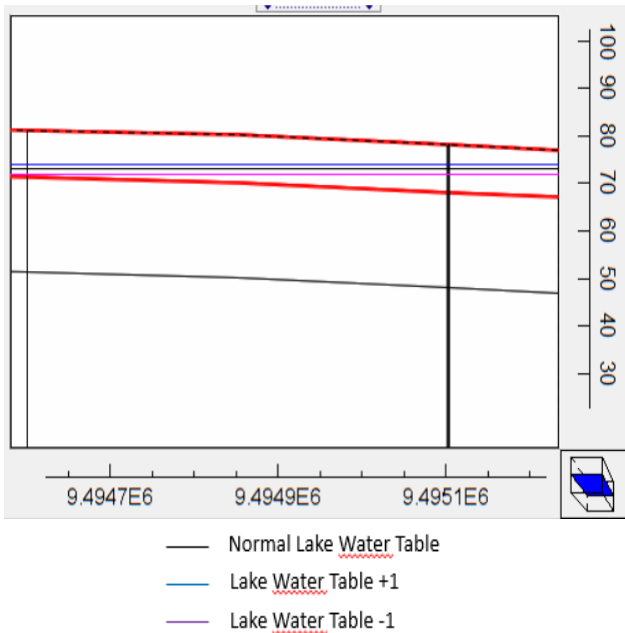


Fig. 9 Interaction section of ground water – lake water +1 (a), normal lake water (b), lake water -1 (c)

The Fluctuation of Lake Water Table- Groundwater Table

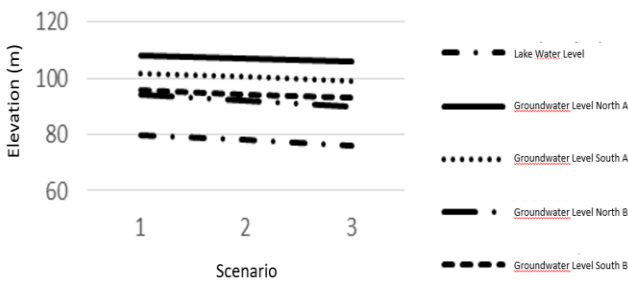


Fig. 10 The ground water – lake water interaction pattern

Based on the numeric simulation carried out, there is found the relation between ground water level and lake water level of Sentani Lake as follows:

$$\text{Fluctuation of ground water level} = 0.1529 \times \text{fluctuation of lake water level} \tag{6}$$

This formulation is obtained through the relationship between the lake water level and the ground water level at the 10 points with the distance of 500 m from the lake (Fig. 11). Additionally, there is carried out the validation test of the model result in relation to the observation result for the other 6 points, and there is determined the good enough correlation coefficient that is 0.97.

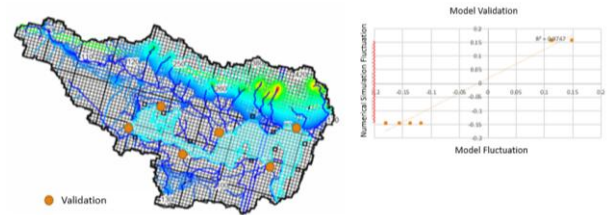
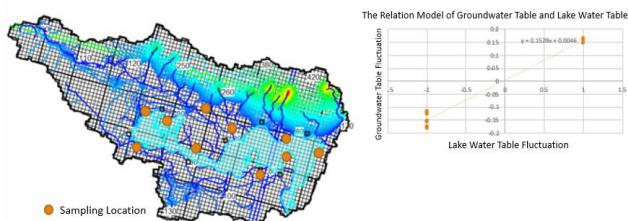


Fig. 11 Sample point for building the model of ground water-ground water and validation point

3.2. Interaction Conceptual Model of Rainfall-Lake Water-Ground Water

The interaction model of rainfall-lake water-ground water is built using the SWAT-MODFLOW. This model studies the interaction of ground water-lake water through the water balance, infiltration pattern, discharge pattern, and contribution of ground water to the inflow of lake water because the factors affect one another. However, the approach that is used by the SWAT model is watershed of river. So, there is taken the sample of watershed that represents the whole condition of geology and geomorphology in surrounding Sentani Lake for analyzing the interaction of rainfall-lake water-ground water in surrounding Sentani Lake.

The more ground water discharge and soil saturation in the Sentani area can be caused by the geology and geomorphology conditions due to the high stone permeability in the downstream, so the ground water in the mountain area of Sentani is big enough to concentrate in the downstream [12]. To evaluate the hypothesis, there is seen the infiltration pattern in surrounding Sentani Lake. Fig. 12 shows that the low infiltration is in the mountains that have frozen and metamorphic stone; however, the high absorption value is in the lowland area with the alluvial lithology. By the high rainfall in the Sentani Lake larea, the infiltration value in the mountains may be caused by the low stone permeability, so there is much water is flowing to the downstream. However, the high infiltration condition in the downstream can cause the saturated ground water condition in the downstream. This implication of the condition causes most of the river stream in surrounding Sentani to be dominated by the overflow of ground water or is usually mentioned as gaining stream.

In the rainy season, there is low absorption in the surroundings of the Cyclops Mountains, so the heavy rainfall is flowing to the downstream. In the dry season, area with the low absorption is widening to the downstream. The concentrated infiltration is only in the downstream near the Sentani Lake. In the rainy season, the rainfall as the overflow of ground water is formed in almost the whole river stream with the discharge is 10,000 until 30,000 m<sup>3</sup> per-day. The catchment area of concentrated ground water is in the middle between downstream and upstream in the dry season. Generally, the river stream is dominated only by the over flow of

ground water; however, the discharge is not as large as in the rainy season. In the downstream area that is waterproof tends to change the rainfall into surface runoff and influences the fluctuation of river discharge (Fig. 12).

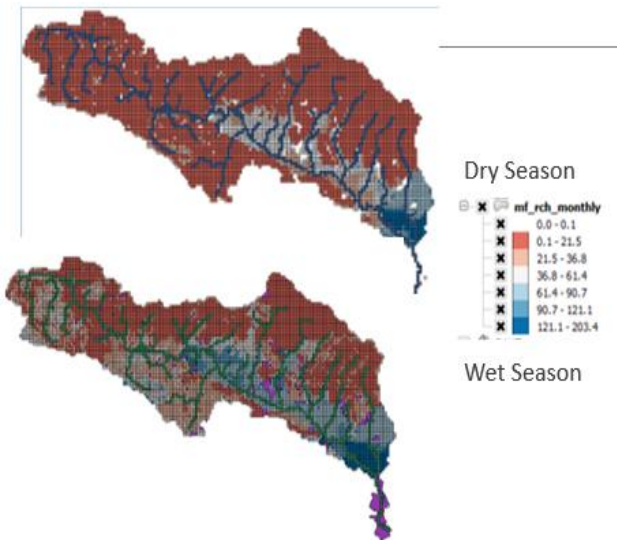


Fig. 12 Distribution of monthly infiltration in the Yahim Watershed

### 3.3. Water Balance of SWAT

To analyze the contribution of groundwater to the Sentani lake water through the hydrograph analysis, we can see the contribution of ground water to the water discharge. The contribution of ground water to the lake water is big enough, 10–15 m<sup>3</sup>/s on average, as presented in Fig. 13.

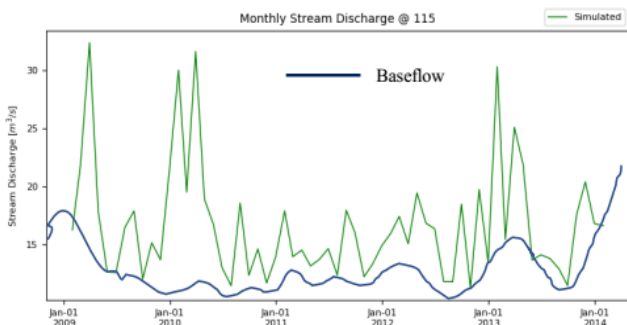


Fig. 13 Monthly discharge of Yahim Watershed

The high base flow shows that the saturation of ground water is in the surrounding locations due to the saturated soil. Most rainfall is difficult to be absorbed into soil and becomes as flood run-off. Through the water balance, as presented in Fig. 14, it is seen that the river flow discharge (green) is dominated by the ground water discharge (old-green), but the ground water discharge tends to be stable form season to season, so when there is an extreme flow discharge, the dominating influencer is rainfall. This condition usually happens in the locations surrounding the mountains because there is more rainfall that is absorbed. Its part leaks and returns to the surface due to the saturated aquifer condition, as presented in Fig. 14.

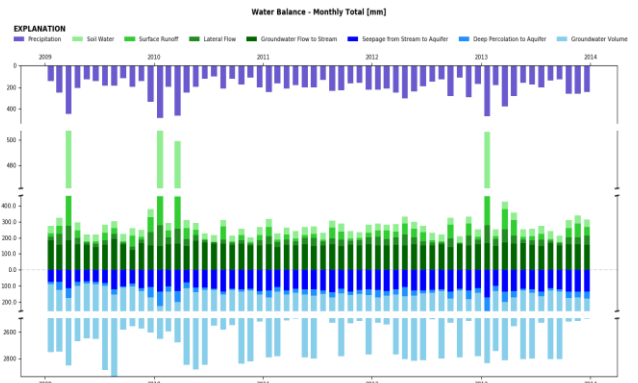


Fig. 14 Balance of rainfall-lake water-ground water

From the analysis of the mudflow budget zone as presented in Fig. 15, the ground water absorbed in the Sentani Watershed accumulates in lake, so the base flow accumulates in Sentani Lake. By combining the ground water and rainfall run-off in the Sentani Watershed, there is known that: Inflow total of lake = Base flow + 0.067 x Rainfall – 5.

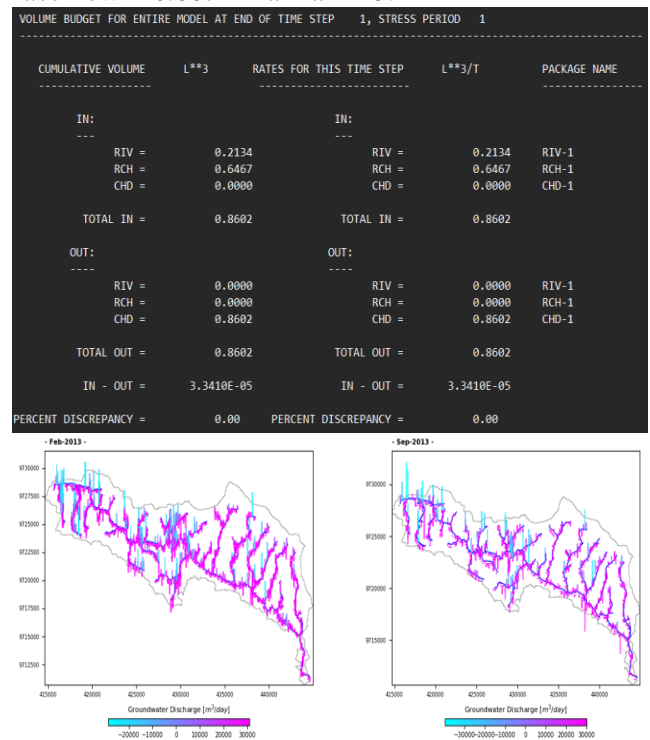


Fig. 15 Interaction of absorption – overflow in the Yahim Watershed

## 4. Conclusion

This research intends to build an interaction model between rainfall, lake water, and ground water by simulating the integration of rainfall-lake water-ground water. The interaction model of rainfall-lake water is built based on the relation between the outlet discharge and rainfall at the 10 points, which is validated by the observation data in 5 points, the model produces the formulation as follows: Rainfall into the lake = 0.067 x rainfall - 5.

The interaction model of lake water level-ground water level is built based on the relation between the

fluctuation of ground water and the lake water level in the 10 points, which is validated to the 6 points. The model produces the following formulation: fluctuation of ground water level =  $0.1529 \times$  fluctuation of lake water level.

By combining the ground water and rainfall run-off in the Sentani watershed, there is known as follows: Inflow total of Lake = base flow +  $0.067 \times$  rainfall - 5. This model is the integration of rainfall-lake water-ground water and it is suitable for the lake that is related to rainfall and ground water.

## References

- [1] MUCHLIS A., BISRI M., LIMANTARA L. M., and SHOLICHIN M. Design Flood of the Mahakam Lake Cascade for Reducing the Flood Downstream. *Journal of Southwest Jiaotong University*, 2021, 56(4): 279-287. <https://doi.org/10.35741/issn.0258-2724.56.4.23>
- [2] SMITH B. D., & ZEDER M. A. The Onset of the Anthropocene. *Anthropocene*, 2013, 4: 8-13. <https://doi.org/10.1016/j.ancene.2013.05.001>
- [3] CHANG Y., HOU K., LI X., ZHANG Y., and CHEN P. Review of land use and land cover change research progress. *IOP Conference Series: Earth and Environmental Science*, 2018, 113: 012087. <http://dx.doi.org/10.1088/1755-1315/113/1/012087>
- [4] CHEN J., LIAO A., CHEN J., PENG S., CHEN L., and ZHANG H. 30-meter global land cover data product- Globe Land30. *Geomatics World*, 2017, 24(1): 1-8.
- [5] JUWONO P. T., LIMANTARA L. M., and AMRIE S. The effect of land use change to the depth and area of inundation in the Bang sub-watershed-Malang-Indonesia. *International Journal of GEOMATE*, 2019, 16(53): 238-244. <http://dx.doi.org/10.21660/2019.53.96946>
- [6] PRIYANTORO D., & LIMANTARA L. M. Conformity Evaluation of Synthetic Unit Hydrograph (Case Study at Upstream Brantas Sub-Watershed, East Java Province of Indonesia). *Journal of Water and Land Development*, 2017, 35: 173-183. <https://doi.org/10.1515/jwld-2017-0082>
- [7] YOHANNES A. W., COTTER M. C., KELBORO G., and DESSALEGN W. Land use and land cover changes and their effects on the landscape of Abaya-Chamo Basin. *Land*, 2018, 7(1): 2. <https://doi.org/10.3390/land7010002>
- [8] HUA W., CHEN H., and SUN S. Assessing climatic impacts of future land use and land cover change projected with the CanESM2 model. *International Journal of Climatology*, 2015, 35(12): 3661-3675. <https://doi.org/10.1002/joc.4240>
- [9] LI G., ZHANG F., and JING Y. Response of evapotranspiration to changes in land use and land cover and climate in China during 2001-2013. *Science of the Total Environment*, 2017, 596-597: 256-265. <https://doi.org/10.1016/j.scitotenv.2017.04.080>
- [10] SANTOS M., & FRAGOSO M. Precipitation thresholds for triggering floods in the Corgo Basin, Portugal. *Water*, 2016, 8(9): 376. <https://doi.org/10.3390/w8090376>
- [11] QUANJIU W., TING Y., YANLI L., GUANGXU Z., and PENGYU Z. Review of Soil Nutrient Transport in Runoff and Its Controlling Measures. *Transactions of the Chinese Society of Agricultural Machinery*, 2016, 47(6): 67-82. <http://nyjxb.net/index.php/journal/article/view/85>
- [12] MARKOVICH K. H., MANNING A. H., CONDON L. E., and MCINTOSH J. C. Mountain-Block Recharge: A Review of Current Understanding. *Water Resources Research*, 2019, 55: 8278-8304. <https://doi.org/10.1029/2019WR025676>
- [13] COUNCIL G. W. *Simulating Lake-Groundwater Interaction with MODFLOW*, 1997. <https://smartech.gatech.edu/bitstream/handle/1853/44196/CouncilG-97.pdf>
- [14] CHENG X., & ANDERSON M. P. Numerical simulation of ground-water interaction with lakes allowing for fluctuating lake levels. *Groundwater*, 1993, 31(6): 929-933. <https://doi.org/10.1111/j.1745-6584.1993.tb00866.x>
- [15] KELBE B. E., & GERMISHUYSE T. The interaction between coastal lakes and the surrounding aquifer. In: SILILO O. (ed.) *Proceedings of the XXX Congress on Groundwater: Past Achievements and Future Challenges*. Balkema, Cape Town, Rotterdam, 2000: 395-400. [https://www.researchgate.net/publication/291629912\\_The\\_Interaction\\_between\\_Coastal\\_Lakes\\_and\\_the\\_surrounding\\_Aquifer](https://www.researchgate.net/publication/291629912_The_Interaction_between_Coastal_Lakes_and_the_surrounding_Aquifer)

## 参考文献:

- [1] MUCHLIS A.、BISRI M.、LIMANTARA L.M. 和 SHOLICHIN M. 为减少下游洪水而设计的玛哈坎湖梯级洪水。西南交通大学学报, 2021, 56(4): 279-287. <https://doi.org/10.35741/issn.0258-2724.56.4.23>
- [2] SMITH B. D. & ZEDER M. A. 人类世的开始。人类世, 2013, 4: 8-13。 <https://doi.org/10.1016/j.ancene.2013.05.001>
- [3] CHANG Y., HOU K., LI X., ZHANG Y., CHEN P. 土地利用与土地覆被变化研究进展综述。眼压系列会议: 地球与环境科学, 2018, 113: 012087。 <http://dx.doi.org/10.1088/1755-1315/113/1/012087>
- [4] CHEN J., LIAO A., CHEN J., PENG S., CHEN L., 和 ZHANG H. 30米全球土地覆盖数据产品——环球大地30。地学世界, 2017, 24(1): 1-8。
- [5] JUWONO P. T.、LIMANTARA L. M. 和 AMRIE S. 土地利用变化对砵子流域-玛琅-印度尼西亚淹没深度和面积的影响。国际GEOMATE杂志, 2019, 16(53): 238-244. <http://dx.doi.org/10.21660/2019.53.96946>
- [6] PRIYANTORO D., & LIMANTARA L. M. 合成单元水位线的符合性评估(印度尼西亚东爪哇省布兰塔斯上游分水岭案例研究)。水与土地开发学报, 2017, 35: 173-183。 <https://doi.org/10.1515/jwld-2017-0082>
- [7] YOHANNES A. W.、COTTER M. C.、KELBORO G. 和 DESSALEGN W. 土地利用和土地覆盖变化以及对阿巴亚查莫盆地景观的理论影响。土地, 2018, 7(1): 2. <https://doi.org/10.3390/land7010002>
- [8] HUA W.、CHEN H. 和 SUN S. 评估未来土地利用和土地覆盖变化的气候影响, 用能无害环境管理2模型预测。国际气候学杂志, 2015, 35(12): 3661-3675。 <https://doi.org/10.1002/joc.4240>
- [9] LI G., ZHANG F., 和 JING Y. 2001-2013年中国土地利用和土地覆被及气候变化对蒸散发的响应。总体环境科学, 2017, 596-597: 256-265. <https://doi.org/10.1016/j.scitotenv.2017.04.080>
- [10] SANTOS M., & FRAGOSO M. 葡萄牙科尔戈盆地引

- 发洪水的降水阈值。水，2016，8(9): 376。  
<https://doi.org/10.3390/w8090376>
- [11] 泉久 W., TING Y., YANLI L., GUANGXU Z., 和 PENGY Z. 径流中土壤养分输送及其控制措施的回顾。中国农业机械学会学报，2016，47(6): 67-82。  
<http://nyjxxb.net/index.php/journal/article/view/85>
- [12] MARKOVICH K. H.、MANNING A. H.、CONDON L. E. 和 MINTOSH J. C. 山块补给：对当前理解的回顾。水资源研究，2019，55: 8278-8304。  
<https://doi.org/10.1029/2019WR025676>
- [13] COUNCIL G. W. 使用模型流模拟湖-地下水相互作用，1997年。  
<https://smartech.gatech.edu/bitstream/handle/1853/44196/CouncilG-97.pdf>
- [14] CHENG X., & ANDERSON M. P. 地下水与湖泊相互作用的数值模拟，允许波动的湖泊水位。地下水，1993，31(6): 929-933。  
<https://doi.org/10.1111/j.1745-6584.1993.tb00866.x>
- [15] KELBE B. E., & GERMISHUYSE T. 沿海湖泊与周围含水层之间的相互作用。在：SILILO O. (编辑) XXX地下水大会论文集：过去的成就和未来的挑战。巴尔科玛，开普敦，鹿特丹，2000：395-400。  
[https://www.researchgate.net/publication/291629912\\_The\\_Interaction\\_between\\_Coastal\\_Lakes\\_and\\_the\\_surrounding\\_Aquifer](https://www.researchgate.net/publication/291629912_The_Interaction_between_Coastal_Lakes_and_the_surrounding_Aquifer)